DOI: 10.13009/EUCASS2017-461

Low order investigation on longitudinal combustion instability in a variable geometry single element combustor

M. L. Frezzotti[♠], *S. D'Alessandro*[♠], *C. Huang*[◇] *and F. Nasuti*[♠]
[♠]*Dipartimento di Ingegneria Meccanica e Aerospaziale, Sapienza Università di Roma*
via Eudossiana 18, 00184, Rome, Italy
[◇]*School of Aeronautics and Astronautics, Purdue University*
701 W. Stadium Ave., West Lafayette, IN, 47907, USA
marialuisa.frezzotti@uniroma1.it · simone.dalessandro@uniroma1.it
huang162@purdue.edu · francesco.nasuti@uniroma1.it

Abstract

Longitudinal high frequency combustion instability is the focus of the present work with particular attention to the CVRC single element combustor, characterized by the variable length of the oxidizer post. Three different geometrical configurations of CVRC combustor are examined and simulated through a quasi-1D Eulerian model, considering three different lengths of the post. The obtained flow field in the three cases is discussed and the limit cycle is described for all the configurations. Qualitative agreement with high fidelity numerical data and experimental data in the literature is obtained, showing marginal instability for the short post configuration and instability for the intermediate and long post. A detailed comparison of limit cycle obtained with high fidelity simulations and quasi-1D analysis is carried out, showing that the latter is characterized by pressure waves of higher intensisty.

1. Introduction

Combustion chambers in liquid rocket engines are characterized by a very high density power and relatively low losses. This feature makes such systems particularly prone to the development of high frequency combustion instability. Such kind of instability is caused by the coupling between unsteady heat release and pressure oscillations. The consequencies can be catastrophic, rapidly yielding to the failure of the engine due to meachanical and thermal loads, resulting in untolerable heat flux. Different operative conditions and geometries end up in different sustaining mechanisms which are hardly predictable or even detectable. Different approaches have been used to gain insights in the phenomenon, both experimental and numerical investigation have been considered in the last decades. Huge full-scale experimental campaigns have been performed in the past[14] with important improvements in the knowledge of the phenomenon. Nevertheless, the costs of such tests are prohibitive to be considered in the development phase of a new system. Nowadays the experimental investigation is mainly carried out on lab-scale combustors.[6–10,13,19] This approach is less expensive and allows to get results in a relatively short time. The scaling procedure does not permit to investigate all the physics occurring in the full-scale engine. Instead, it has to be carried out according to the specific requirements to be met to focus on a specific aspect of the system behavior.[3,4] In this framework, numerical simulations are necessary to support experimental activities, limiting the number of tests and giving information about quantities that are difficult to be directly measured, such as heat flux or heat release.

As far as numerical simulations are concerned, two main approaches are currently pursued: high fidelity simulations and low order models. On one hand, high fidelity simulations, such as Direct Numerical Simulations (DNS), Large Eddy Simulations (LES) or Detached Eddy Simulations (DES), reproduce the flow field in detail and are usually capable of capturing the main physical aspects. Unfortunately they require huge computational effort that becomes prohibitive for full-scale analyses. On the other hand, low order models are capable of giving quick evaluations of the system behavior, replacing detailed mechanisms with suitable models. For example, in the present case of high frequency combustion instability, the coupling between acoustics and combustion and all the related phenomena are described through a response function, i.e. a source term in the energy equation accounting for pulsing heat release rate, as shown in the following section.

The present work focuses on longitudinal high frequency combustion instability, with particular attention to a specific single element combustor, the Continuously Variable Resonance Combustor (CVRC), designed and installed

DOI: 10.13009/EUCASS2017-461

at Purdue University.[18,19] The peculiar characteristic of the CVRC is the presence of an actuator capable of varying the position of the choked point in the oxidizer post and, consequently, its effective length, from 9 cm to 19 cm. During the test this displacement yields self-excited combustion instability for a given range of the post length. Even in this lab-scale test, the high fidelity approach is still quite expensive in terms of computational cost.[10,16] Given these considerations, it seems reasonable to look for reliable low-order models to investigate their capability of predicting unstable behavior. In particular, in this work a quasi-1D Eulerian model is considered and a response function of the $n-\tau$ family[2] is implemented to model the unsteady heat release rate. Generally speaking the qualitative or quantitative evaluation of response functions has to be based on experimental or high fidelity simulations data.[1,11] and in this case it is carried out on the basis of 2D-axisymmetric DES simulations performed at Purdue University.[16]

The aim of the present work is to use the quasi-1D approach of Frezzotti et al.[5] to study three different geometrical configurations of CVRC: a short post (L_{op} = 9 cm), intermediate post (L_{op} = 14 cm) and a long post (L_{op} = 19 cm) configuration (referred to as SPC, IPC and LPC, respectively). The generality of the approach for the selected combustor is verified, independently of the oxidizer post length L_{op}. The SPC exhibits marginal instability while the IPC is unstable and the LPC is in a region of post lengths where experiments have shown both stable and unstable conditions.

2. Governing equations and quasi-1D modeling

A solver of multispecies quasi-1D Euler equations has been developed with the aim of including nonlinear regime in the study of combustion instability through simplified tools according to Smith et al.[17] In order to describe the physics of CVRC, combustion has to be taken into account. First of all, in order to satisfy the mass balance, it is necessary that

$$\dot{\omega}_p - \dot{\omega}_o = \dot{\omega}_{fu} \tag{1}$$

where $\dot{\omega}_p, \dot{\omega}_o$ and $\dot{\omega}_{fu}$ are the rate of production per unit length of combustion products, oxidizer and fuel, respectively. In fact, combustion products are considered as a single species whose properties are computed with the chemical equilibrium code CEA[12] and corrected for taking into account the effect of temperature on c_p (specific heat at constant pressure) that is not considered in the model. Eq.(1) can be expressed as a function of the OF ratio, i.e. the ratio between oxidizer and fuel mass flow rate

$$\dot{\omega}_p = \dot{\omega}_o \left(1 + \frac{1}{OF}\right) \tag{2}$$

As shown in eq.(2), $\dot{\omega}_p$ and $\dot{\omega}_{fu}$ are both functions of $\dot{\omega}_o$. In order to simplify the model, only two species are considered: oxidizer and combustion products. Oxidizer is introduced at the left boundary (Fig. (1)) and consumed within a finite region of the chamber, identified by the abscissas l_s and l_f, where combustion is supposed to occur. In this zone of the chamber oxidizer is consumed and replaced by combustion products, according to the proportion given in eq.(2). Fuel is supposed to be injected in the region between l_s and l_f where it reacts instantaneously. In particular, as previously shown, production rates can be expressed as functions of $\dot{\omega}_o$ that is modeled as

$$\dot{\omega}_o = \beta \frac{\dot{m}_o}{l_f - l_s} Y_o(x,t) s(x) \tag{3}$$

where $\dot{m}_o$ is the oxidizer mass flow rate, $Y_o(x,t)$ is the oxidizer mass fraction, β is the minimum scalar value that allows to consume all the oxidizer in the space of the selected finite length combustion zone ($l_f - l_s$) at steady state and $s(x)$ is a sinusoidal shape function defined between the abscissas l_s and l_f (see Fig. (1)) and it is introduced to avoid discontinuities in the source terms.

Governing equations can be easily derived starting from continuity equation

$$(\rho A)_t + (\rho u A)_x = \dot{\omega}_p - \dot{\omega}_o \tag{4}$$

where ρ and u are mixture density and velocity, A is cross sectional area. The second equation is continuity for the oxidizer

$$(\rho A Y_o)_t + (\rho u A Y_o)_x = -\dot{\omega}_o \tag{5}$$

where the minus sign at the right hand side suggests that the source term is actually a consumption term. The last two equations are momentum and energy balances

$$(\rho u A)_t + \left[\left(\rho u^2 + p\right) A\right]_x = p A_x + u(\dot{\omega}_p - \dot{\omega}_o) \tag{6}$$

$$(\rho e_0 A)_t + (\rho u h_0 A)_x = (\dot{\omega}_p - \dot{\omega}_o)\left(h_0 + OF \Delta h_0^{rel}\right) + \dot{q}_{us} \tag{7}$$

DOI: 10.13009/EUCASS2017-461

where e_0 and h_0 are total internal energy and total enthalpy which include the kinetic energy $u^2/2$ and are linked to pressure and density via the perfect gas relationship ($R = \sum R_i Y_i, c_p = \sum c_{p_i} Y_i$ and $\gamma = c_p/(c_p - R)$ with c_p and c_v specific heat at constant pressure and volume, respectively and R gas constant), Δh_0^{rel} is the heat of reaction per unit mass of oxidizer, released by chemical reactions. The term $\dot{q}_{us}$ refers to unsteady heat release contribution. More precisely, it represents the response function through which the model takes into account the effect of flow field oscillations on combustion. This effect is modeled according to[2] expressing the unsteady part of heat release as function of velocity (eq.(8)) sampled at a specific abscissa (x_u, almost coincident with the antinode of the first longitudinal modal shape), with a certain time-lag τ, for velocity time-lag formulation.

$$\dot{q}_{us}(x,t) = \frac{e^{-\frac{(x-\mu)^2}{2\sigma^2}}}{\sqrt{2\pi\sigma^2}} \alpha \, A(x) \; [u(x_u, t-\tau) - \bar{u}(x_u)] \tag{8}$$

The overlined values are the time averaged values, μ and σ are mean value, standard deviation of the Gaussian distribution assumed as shape function (Fig. (1)) for the velocity time lag response to avoid discontinuities in the unsteady heat release source term and emphasize its statistical aspect. The selected shape function allows one to select a given "combustion" profile in a well defined region.[17] The amount of heat released due to pressure or velocity oscillation is controlled by a proportionality factor of response function intensity α , in analogy with the interaction index n in Crocco's $n - \tau$ formulation. Figure (1) shows the geometry, assumed for the quasi-1D computation, and the shape functions associated to the different source terms. Boundary conditions are fixed oxidizer mass flow rate ($\dot{m}_{o,0}$) and stagnation temperature (T_0) at the inlet and a choked nozzle with a supersonic outflow.

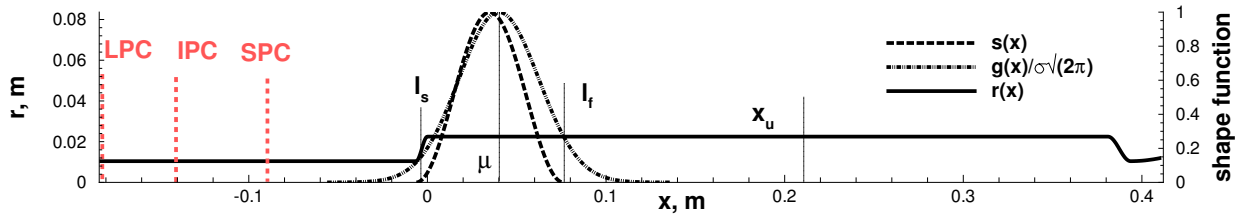

Figure 1: CVRC computational domain. Mass source term shape function $s(x)$, bounded between the abscissas l_s and l_f, Gaussian distribution associated to response function $g(x)$, velocity sampling location x_u. The labels LPC, IPC and SPC mark the length of the post for the three configurations.

3. Response function calibration

The response function characteristic parameters have been inferred by the results of the two-dimensional simulations performed by Sardeshmukh et al.[16] The flow field given by DES results has been averaged in the cross-section for consistency with the quasi-1D model, where the response function is implemented. In particular, the sampling location x_u has been chosen at the velocity antinode of the first longitudinal mode occurring in the middle of the chamber. The time lag has been estimated evaluating the cross-correlation between the signal of velocity at x_u and the heat release rate integrated in the chamber. It represents the distance in time between the peak of velocity at the sampling location and the peak of heat release rate. The mean of the Gaussian distribution, μ, has been selected as the location of maximum heat release rate while σ has been calibrated fitting the Gaussian distribution on the standard deviation of heat release rate oscillations of DES simulations. The phase average process is particularly useful for periodic phenomena affected by cycle-to-cycle variations. In the present test case, in particular, phenomena such as turbulence and chemical reactions introduce disturbances that affect the periodicity of the limit cycle. Moreover, not only the amplitude but also the period of each cycle is slightly variable in time. For such cases, Ostermann et al.[15] suggest a particular procedure in order to perform the phase average. First of all, the period of each cycle is evaluated through the auto-correlation method, where a segment of the reference velocity signal is correleated with a shifting fragment of the same signal. The optimum length for the segment is between 0.5 and 1.0 of mean period length, as reported by Ostermann et al.[15] To obtain a phase averaged signal, a suitable angle range (window) must be defined. The choice of the window results from a trade-off between the necessity of limiting the signal noise and the need of preserving inherent flow characteristics. The used optimization criterion consists in computing and minimizing the root mean sqaure (RMS) of the difference between the reference signal and the phase averaged cycle. The optimized phase window results to be equal to 4 deg. As far as the response function evaluation is concerned, the main purposes of the

DOI: 10.13009/EUCASS2017-461

phase averaging consists in estimating the proportionality index, α, as the ratio between the peak to peak amplitude of phase averaged heat release rate and velocity oscillation. For the sake of clarity, the computed phase average signals are shown in Fig. (2) for the IPC configuration, while the whole sets of estimated parameters are summarized in Table 1.

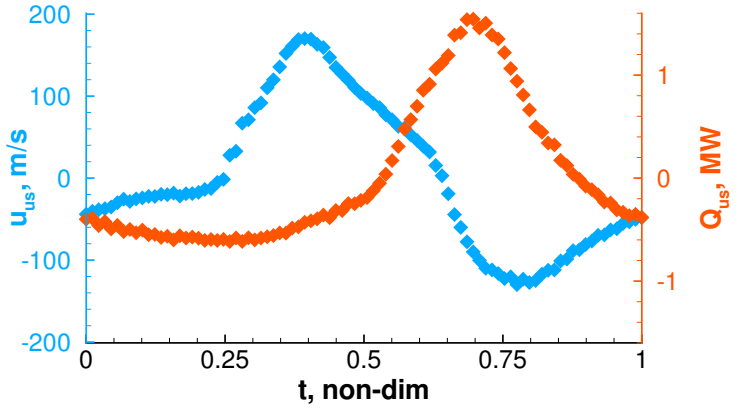

Figure 2: Phase averaged velocity and heat release rate fluctuations in the IPC.

Table 1: Response function characteristic parameters for the three selected geometrical configurations of CVRC.

	α, kPa/m	τ, ms	μ, m	σ, m	x_u, m
SPC	5653.3	0.41	0.0360	0.0367	0.242
IPC	3894.2	0.48	0.0355	0.0358	0.215
LPC	3613.1	0.49	0.0385	0.0386	0.215

As can be observed from Table 1, the parameters are very similar in all the configurations with the only exception of α, the proportionality index. In fact, for the SPC case its magnitude is significantly higher with respect to the other configurations. Due to the less pronounced coupling characterizing this configuration, the fluctuations of heat release rate have a lower effect on the velocity oscillations, resulting in a higher ratio between the peak to peak amplitude of the averaged signals.

4. Results and Discussion

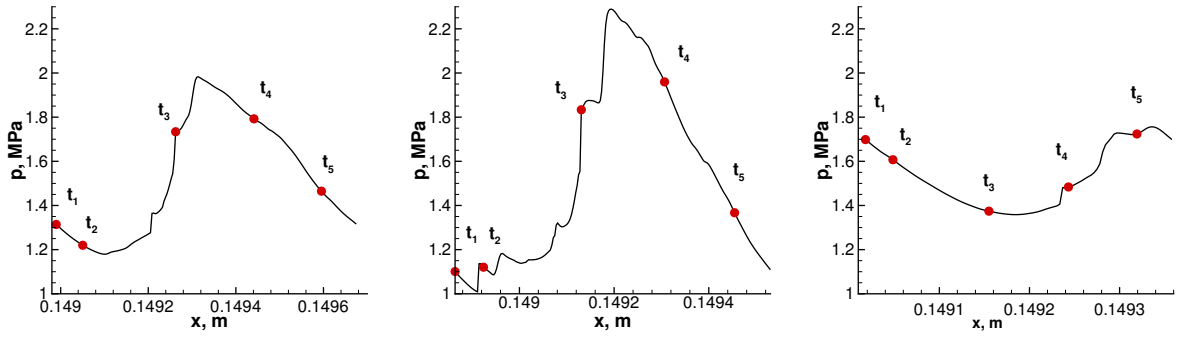

(a) *LPC* (b) *IPC* (c) *SPC*

Figure 3: Limit cycle description for the three configurations of CVRC. Pressure sampled at $x = 0.368$ m

The computed pressure at the nozzle entrance ($x = 0.368$ m) is reported in Fig. (3) for the three configurations. The main features of limit cycle are then discussed using the obtained temperature, pressure and velocity behaviors, shown in Fig. (4), at different times within one cycle for the three configurations. The shown snapshots, from t_1 to

DOI: 10.13009/EUCASS2017-461

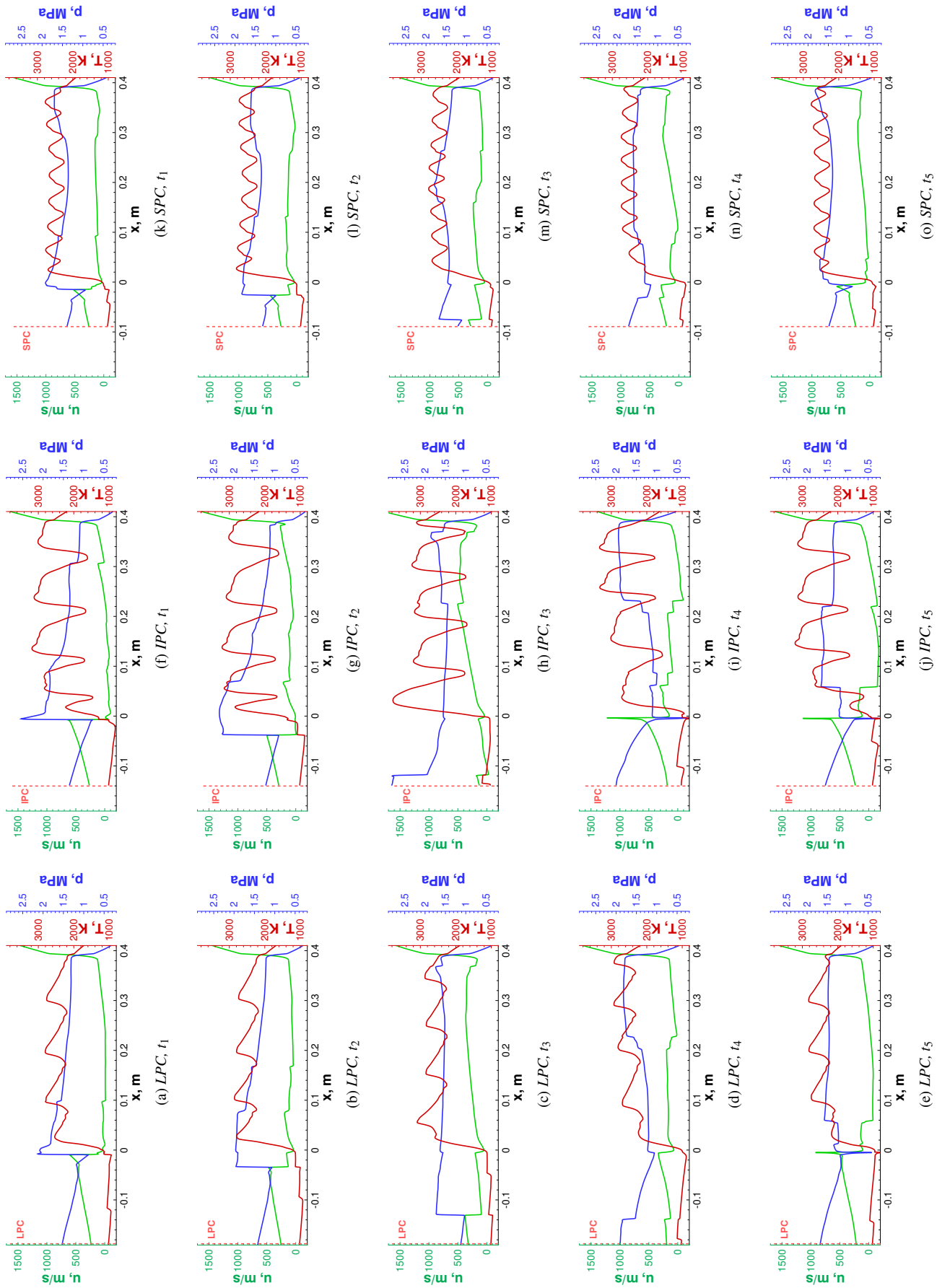

(a) *LPC*, t_1 (b) *LPC*, t_2 (c) *LPC*, t_3 (d) *LPC*, t_4 (e) *LPC*, t_5

(f) *IPC*, t_1 (g) *IPC*, t_2 (h) *IPC*, t_3 (i) *IPC*, t_4 (j) *IPC*, t_5

(k) *SPC*, t_1 (l) *SPC*, t_2 (m) *SPC*, t_3 (n) *SPC*, t_4 (o) *SPC*, t_5

Figure 4: Limit cycle description for the three configurations of CVRC, from left to right, LPC, IPC and SPC respectively.

DOI: 10.13009/EUCASS2017-461

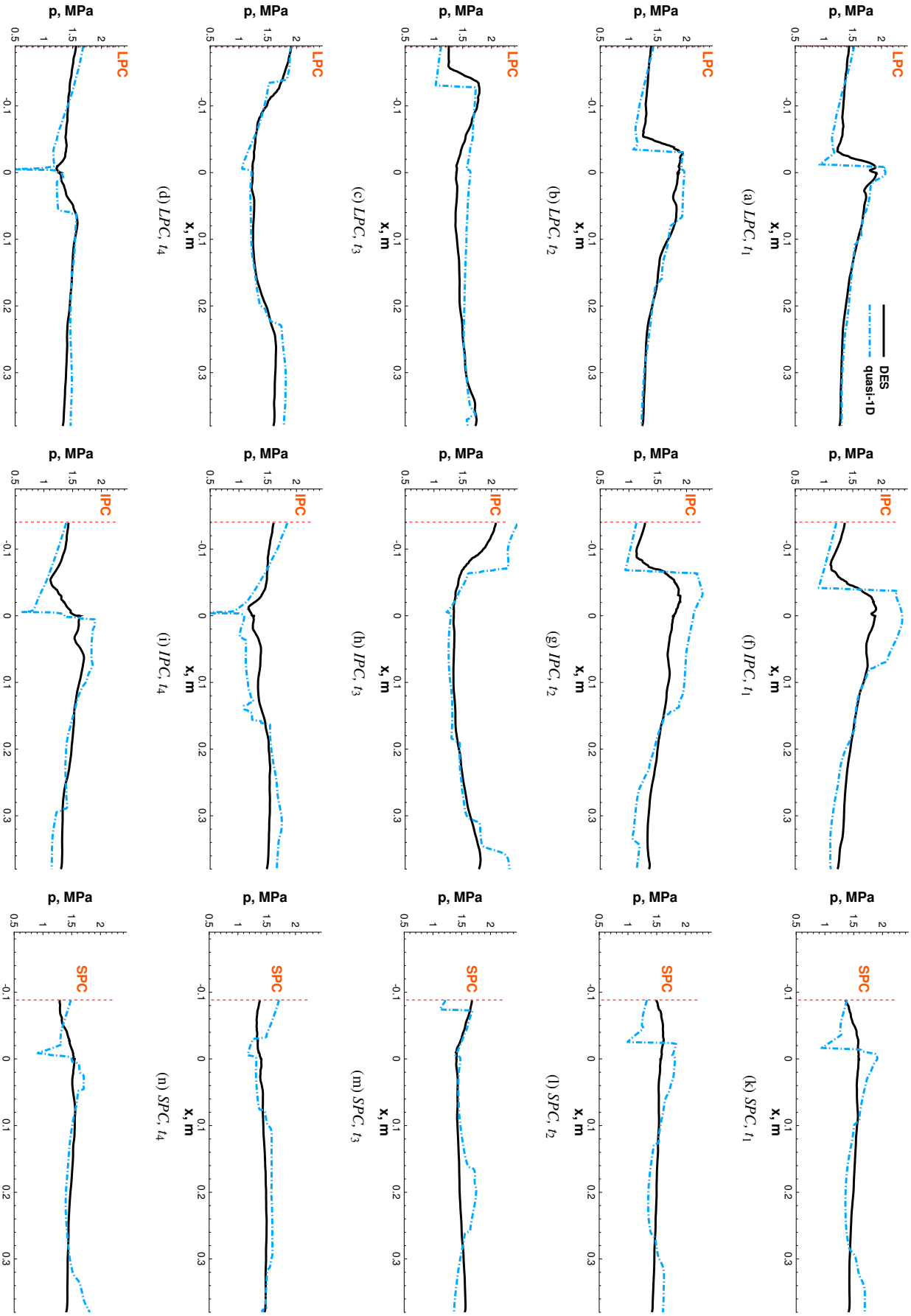

Figure 5: Pressure at limit cycle. Comparison between DES and quasi-1D results for the three configurations of CVRC.

DOI: 10.13009/EUCASS2017-461

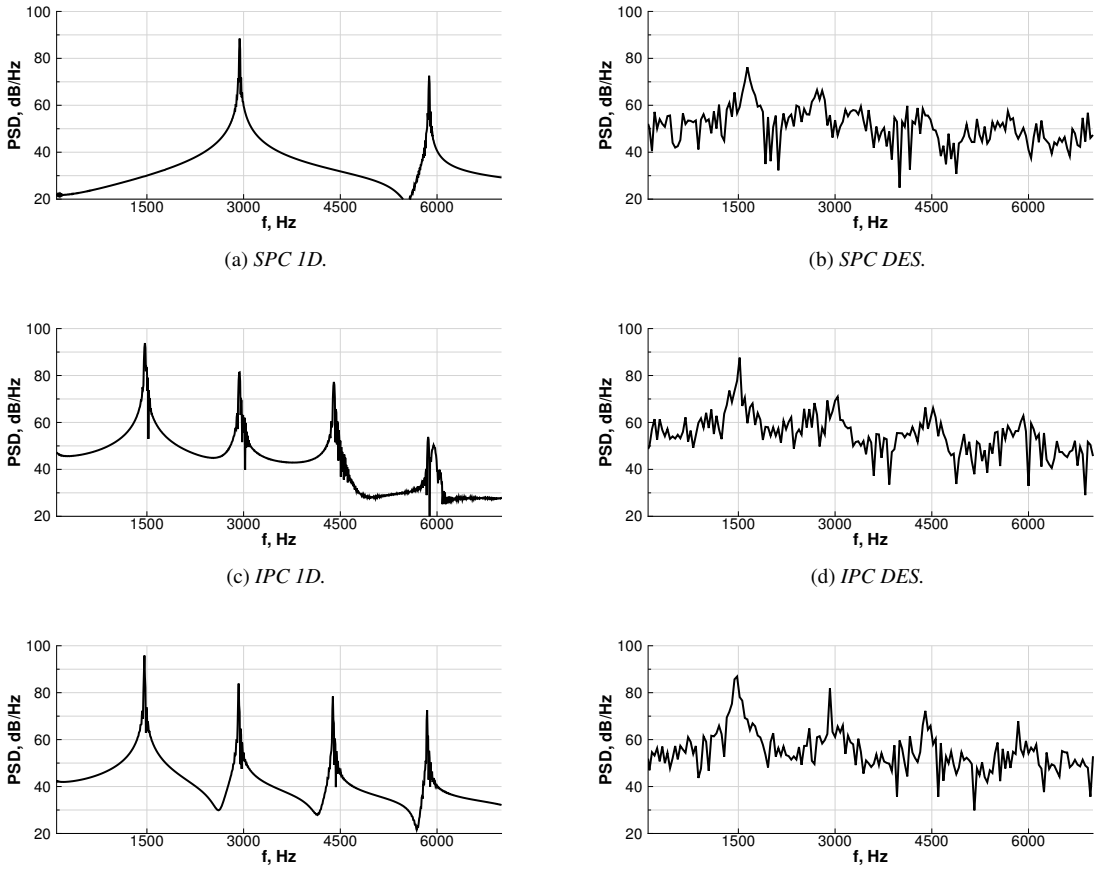

(a) *SPC 1D.* (b) *SPC DES.*

(c) *IPC 1D.* (d) *IPC DES.*

(e) *LPC 1D.* (f) *LPC DES.*

Figure 6: Power spectral density of pressure. Comparison between quasi-1D and DES results for the three configurations.

DOI: 10.13009/EUCASS2017-461

t_5 correspond to the times pointed out in Fig. (3) representing the pressure signal sampled just upstream the nozzle entrance.

In the LPC, t_1 (Fig. (4a)) corresponds to the maximum pressure at the step, i.e. the area variation at $x = 0$ m, due to a shock wave moving upstream and reflecting a shock as a consequence of the interaction with the geometrical discontinuity (t_2, Fig. (4b)). At time t_3 (Fig. (4c)) the shock waves continue propagating in the post and in the chamber, respectively, until the reflection at the left boundary, for the first, and at the nozzle, for the second, occurs (t_4, Fig. (4d)). The snapshot at time t_5 (Fig. (4e)) shows the interaction between the reflected waves that reach the step at, approximately, the same time. The shock traveling downstream from the post reflects a rarefaction wave (which is in fact visible in t_1 (Fig. (4a)), where the cycle starts again) that is rapidly canceled by the shock moving upstream from the chamber.

The IPC is characterized by similar features with respect to the LPC. In particular at t_1 (Fig. 4f) the shock crossing the step produces a reflected shock traveling in the chamber as in the previous case. A similar scenario, compared to LPC, is observed until t_3 (Fig. (4h)) when the two shocks reflection at the left boundary in the post and at the nozzle occurs roughly at the same time. At time t_4 and t_5 (Figs. (4i) and (4j)) a transonic rarefaction wave is reflected by the shock traveling downstream when passing through the cross-sectional area variation.

Finally, the SPC is considered. Time t_1 and t_2 (Figs. (4k) and (4l) respectively) show the presence of three shock waves in the combustor, one traveling upstream and crossing the step, as in the previous cases, and the other two, generated on different characteristic family, moving in the chamber in opposite directions. At time t_3 (Fig. (4m)) the shock in the post is almost reaching the left boundary while the interaction of the two shocks in the middle of the chamber produces, again, two shocks of opposite characteristic family. At time t_4 (Fig. (4n)) the shock in the post has been reflected and at time t_5 (Fig. (4o)) it is passing through the area variation, reflecting a rarefaction wave. The main difference with the previous configurations is that, within one cycle, the shocks moving in the chamber experience not only the interaction with the area variation at the step and at the nozzle entrance but also an interaction between the shocks at about $x = 0.22$ m. The main consequence is that for the LPC and IPC the limit cycle main frequency is at 1450 Hz while for the SPC it is 2950 Hz, as shown in Fig. (6) where the power spectral density (PSD) of pressure obtained with quasi-1D modeling is compared to the DES results. A summary of limit cycle amplitude and main frequency given by experiments, multi-dimensional simulations and quasi-1D results is given in Table 2.

Furthermore, a detailed comparison between phase averaged fields, obtained from quasi-1D analysis and DES results averaged in the cross-section, is presented in Fig. (5). The quasi-1D model overestimates the intensity of pressure waves for all the configurations, even if the overall acoustic behavior is well captured. The influence of this feature is maximum in the case of SPC where the two models predict different frequencies. In particular, the cycle in the quasi-1D model occurs at the second longitudinal resonance frequency while the first frequency is dominant in DES results. Moreover, the DES results for the SPC are characterized by weak pressure waves that can be hardly identified especially after applying the average procedures. In particular, the snapshot from t_1 to t_5 for the SPC in Fig. (5) show that when the compression in the post crosses the area variation moving downstream, the transmitted pressure wave is almost of null intensity while this is not the case for quasi-1D. The presence of such wave is at the basis of the interaction occurring in the middle of the chamber (Fig. (4m)) that is capable of driving the excitation on the second resonant frequency. Part of this mismatch can be due to the assumption made on heat release rate distribution. In fact, for the SPC case, that is more stable with respect to the other configurations, heat relase occurs in a more spread region of the chamber and with less organized fluctuations. This might suggest the necessity for a more detailed description of heat release rate in space to correctly capture the overall behavior and the observed dominant frequency. In this sense, the high value of α reported in Table 1 for the SPC highlights the need for a more sophisticated response model, capable of capturing the stable behavior.

The limit cycle is quantitatively well captured in the LPC configuration with the exception of the shock wave at the step in Fig. (5a) and of the rarefaction wave in Fig. (5e). In the IPC a similar scenario can be observed. Figures from (5f) to (5j) show that the correct gasdynamic field is predicted by the quasi-1D analysis but the magnitude of waves is overestimated, especially in the region of the post. For all the considered configurations, the wave fronts result to be steeper in the quasi-1D model than in DES results where dissipative effects are of higher intensity.

In terms of the overall physics description, the quasi-1D model cannot describe in detail the mechanism sustaining instability where, for example, vorticity and fuel accumulation in the step region play a fundamental role.[10] Nevertheless, the model reproduces the correct effect of geometrical variations on stability. In fact, the system of waves observed in the quasi-1D model and the characteristic times of propagation are deeply related to the variable length of the oxidizer post that is the main feature producing different regimes for the three configurations. The capability of the quasi-1D model of capturing the correct overall behavior is justified considering the hypotheses governing the response function model. In fact, the $n - \tau$ respose model is based on the assumption that all the phenomena sustaining instability can be related to fluctuations of the selected acoustic variable.[2] From the physical point of view, this is actually the case, since the intermittency of fuel flow in the chamber, described by Harvazinski et al.,[10] is due to the adverse

DOI: 10.13009/EUCASS2017-461

pressure gradient and a pulsing heat release rate is observed, as a consequence. In conclusion, even if the quasi-1D model is characterized by a quite high level of simplification, neglecting important factors such as three-dimensional effects, turbulence and chemical kinetics, it results to be consistent with the main features of the combustor physics.

Table 2: Comparison of limit cycle peak-to-peak (ptp) amplitude and main frequency from experiments[10,16] 2D simulations[16] and quasi-1D results.

	Experiments			2D RANS-LES			Quasi-1D		
	LPC	IPC	SPC	LPC	IPC	SPC	LPC	IPC	SPC
Amplitude (ptp), MPa	0.65	0.63	0.35	0.70	0.80	0.35	0.70	1.30	0.40
Frequency, Hz	1276	1337	1379	1480	1520	1640	1450	1450	2950

5. Conclusion and perspective

A single element combustor with variable length of the oxidizer post is investigated using both DES and quasi-1D modeling. A comparison between the two approaches has been carried out. The behavior observed with quasi-1D modeling is a good representation of the reference DES results and of experiments reported in the literature in terms of qualitative agreement, showing self-excited instability at the first longitudinal frequency for LPC and IPC. The marginal instability of the SPC is actually well represented in terms of oscillation amplitude. The quasi-1D frequency content, in this case, is mainly represented by the second longitudinal resonant frequency, in contrast with the DES data where the first longitudinal frequency results to be dominant. Nevertheless it has to be remarked that the SPC is marginally unstable in both experiments and high fidelity simulations, showing a limit cycle of limited amplitude and less organized pressure fluctuations. As a consequence, the dominant frequencies can be identified but the associated density of power is weaker with respect to the other test cases. In terms of description of the physics occurring in the combustor, where the instability is mainly related to irregular flow of fuel in the chamber and consequent pulsing burning, the quasi-1D description is obviously not capable of capturing these events but it is nevertheless capable of generating a system of waves producing the same overall effect of high pressure fluctuations.

References

[1] L. T. W Chong, S. Bomberg, A. Ulhaq, T. Komarek, and W. Polifke. Comparative validation study on identification of premixed flame transfer function. *Journal of Engineering for Gas Turbines and Power, Volume 134*, 2012.

[2] L. Crocco and S.I. Cheng. *Theory of Combustion Instability in Liquid Propellant Rocket Motors*.

[3] M. L. Dranovsky. *Combustion Instabilities in Liquid Rocket Engines. Testing and Development Practices in Russia*. V. Yang, F. E. Culick, D. G. Talley, Progress in Aeronautics and Astronautics.

[4] S. C. Fisher, F. E. Dodd, and R. J. Jensen. Scaling techniques for liquid rocket combustion stability testing. In V. Yang and W. E. Anderson, editors, *Liquid Rocket Engine Combustion Instability*, volume 169 of *Progress in Aeronautics and Astronautics*, chapter 21, pages 545–564. AIAA, 1995.

[5] M. L. Frezzotti, F. Nasuti, C. Huang, C. L. Merkle, and W. E. Anderson. Determination of heat release rate response function from 2d hybrid rans-les data for the cvrc combustor. 51st AIAA/ASME/SAE/ASEE Joint Propulsion Conference, July 2015, Orlando, FL.

[6] S. Gröning, J. S. Hardi, D. Suslov, and M. Oschwald. Analysis of phase shift between oscillations of pressure and flame radiation intensity of self-excited combustion instabilities. 6th European Conference for Aeronautics and Space Sciences, June 29th - July 3rd 2015, Krakow, Poland.

[7] S. Gröning, D. Suslov, J. S. Hardi, and M. Oschwald. Influence of hydrogen temperature on the acoustics of a rocket engine combustion chamber operated with lox/h2 at representative conditions. Space Propulsion Conference, May 2014, Cologne, Germany.

[8] S. Gröning, D. Suslov, M. Oschwald, and T. Sattelmayer. Stability behaviour of a cylindrical rocket engine combustion chamber operated with liquid hydrogen and liquid oxygen. 5th European Conference for Aeronautics and Space Sciences, July 2013, Munich, Germany.

DOI: 10.13009/EUCASS2017-461

[9] J. S. Hardi, M. Oschwald, and B. B. Dally. Study of lox/h2 spray flame response to acoustic excitation in a rectangular rocket combustor. 49th AIAA/ASME/SAE/ASEE Joint Propulsion Conference, July 2013, San Jose, CA.

[10] M. E. Harvazinski, C. Huang, V. Sankaran, T. W. Feldman, W. E. Anderson, C. L. Merkle, and D. G. Talley. Coupling between hydrodynamics, acoustics and heat release in a self-excited unstable combustor. *Physics of Fluids, Vol. 27, 045102*, 2015.

[11] H. J. Krediet, C. H. Beck, W. Krebs, S. Schimek, C. O. Paschereit, and J. B. W. Kok. Identification of the flame describing function of a premixed swirl flame from les. *Combustion Science and Technology, vol. 184, pp. 888-900*, 2012.

[12] B. J. McBride and S. Gordon. Computer program for calculation of complex chemical equilibrium compositions and applications. Technical Report 1311, 1994. NASA Reference Publication.

[13] K. Miller, J. C. Sisco, N. Nugent, and W. E. Anderson. Combustion instability with a single-element swirl injector. *Journal of Propulsion and Power, Vol. 23, pp. 1102-1112*, 2007.

[14] J. C. Oefelein and V. Yang. Comprehensive review of liquid-propellant combustion instabilities in f-1 engines. *Journal of Propulsion and Power, Vol. 9, No. 5, September-October*, 1993.

[15] F. Ostermann, R. Woszidlo ans C. N. Nayeri, and C. O. Paschereit. Phase-averaging methods for a natural flowfield of a fluidic oscillator. *AIAA Journal*, 53(8):2359–2368, 2015.

[16] S. V. Sardeshmukh, W. E. Anderson, M. E. Harvazinski, and V. Sankaran. Prediction of combustion instability with detailed chemical kinetics. 53th AIAA Aerospace Science Meeting, January 2015, Kissimmee, FL.

[17] R. Smith, M. Ellis, G. Xia, V. Sankaran, W. Anderson, and C. L. Merkle. Computational investigation of acoustics and instabilities in a longitudinal-mode rocket combustor. *AIAA Journal, Vol. 46, No. 11, November*, 2008.

[18] Y. C. Yu. *Experimental and analytical Investigations of Longitudinal Combustion Instability in a Continuously Variable Resonance Combustor (CVRC)*. PhD thesis, Purdue University, School of Aeronautics and Astronautics, 2009.

[19] Y. C. Yu, J. C. Sisco, W. E. Anderson, and V. Sankaran. Examination of spatial mode shapes and resonant frequencies using linearized euler solutions. 2007. 37th AIAA Fluid Dynamich Conference & Exhibit, 25-28 June, Miami, FL.